Available online at www.sciencedirect.com
ScienceDirect
Journal of Solid State Chemistry 181 (2008) 2113–2116
JOURNAL OF SOLID STATE CHEMISTRY
www.elsevier.com/locate/jssc

Rapid communication

Density functional study on electronic properties of P-doped spinel silicon carbon nitride

Yufen Zhang[a], Xian Zhao[a,*], Xiufeng Cheng[a], Yuguang Mu[b,**]

[a]State Key Laboratory of Crystal Materials, Shandong University, Jinan 250100, PR China
[b]School of Biological Science, Nanyang Technology University, Nanyang Drive 60, Singapore 637551, Singapore

Received 2 August 2007; received in revised form 2 November 2007; accepted 12 November 2007
Available online 22 November 2007

Abstract

We performed density functional calculations on the electronic properties of P-doped spinel silicon carbon nitride. When Si is replaced by C at the tetrahedral sites of P-doped c-Si_3N_4, the band gap can be adjusted, and an insulator-to-metal transition is predicted to occur at the C-to-Si ratio of 0.27. Finally, some possible examinations and potential applications for the large band-gap reduction are discussed.
© 2007 Elsevier Inc. All rights reserved.

Keywords: DFT; Electronic properties; Insulator-to-metal transitions; P-doped spinel nitrides

1. Introduction

The discovery of spinel silicon nitride (c-Si_3N_4) with high temperature metastability and the other spinel nitrides provides a new class of solid-state materials, which have attracted many experimental [1–7] and theoretical [8–12] investigations for its outstanding mechanical, electronic, and thermal properties [1–7,13]. c-Si_3N_4, as well as spinel carbon nitride, was predicted to be a wide-band-gap semiconductor by first-principles calculations [1,8,10], whose electro-optic properties are comparable to those of GaN [6]. It is well known that very low concentrations of substitutional P in GaN have a profound effect on the electronic properties [14–16]. So, it can be speculated that incorporation of low concentrations of P impurity in either c-Si_3N_4 or spinel silicon carbon nitride (donated c-Si_3N_4:P, c-$(Si,C)_3N_4$:P) could induce a different electronic structure with drastically altered physical properties that may lead to new applications. It is therefore timely to investigate the electronic structure of these systems. The method of density functional theory (DFT) has been successfully used in predicting crystal structures and properties of group-IV nitrides [8–11]. In this paper, we carried out first-principles calculations based on DFT to investigate the interesting electronic properties of c-$(Si,C)_3N_4$:P. We hope that such calculations could provide more insights into the relation between the structure and the properties for this spinel nitride.

2. Computational method and details

The first-principles electronic structure calculations based on DFT [17] within CASTEP 4.1 code [18] were carried out to determine the stability and electronic properties of the solid solution between spinel Si_3N_4 and C_3N_4. The Vanderbilt ultrasoft pseudopotential [19] with generalized gradient approximation due to Perdew Burke Ernzerhof (GGA-PBE) [20] for exchange-correlation effects was used to model our systems. A cutoff energy of 310 eV for Si_3N_4–C_3N_4 (280 eV for Si_3N_4–Ge_3N_4) in the plane wave expansion was employed in the calculations. A $4\times4\times4$ Monkhorst–Pack grid [21] was used for integration over the irreducible part of the Brillouin zone of the ternary spinel nitrides. For P-doped nitrides, a $3\times3\times3$ Monkhorst–Pack grid was used. Good convergence was achieved with these cutoff energies and number of k points.

*Corresponding author. Fax: +86 531 88366330.
**Also to be corresponded to.
E-mail addresses: zhaoxian@icm.sdu.edu.cn (X. Zhao), YGMu@ntu.edu.sg (Y. Mu).

0022-4596/$ - see front matter © 2007 Elsevier Inc. All rights reserved.
doi:10.1016/j.jssc.2007.11.017

To explore the electronic properties of these solid solutions, we employed a 56-atom supercell (the full cubic spinel cell) and a 112-atom supercell (containing $2\times2\times2$ primitive cells) with the starting configuration of c-Si_3N_4 suggested in Ref. [8]. We substituted Si atoms by C (or Ge), then substituted one P atom with N to model single substitutional P neutral impurity (P atoms on the N sites, donated P_N) in spinel nitrides, the resulting supercells are $C_xSi_{24-x}N_{32}$ ($x=1, 4, 20$), $Ge_xSi_{24-x}N_{32}$ ($x=4, 20$), $Si_{24}N_{31}P$, and $C_xSi_{48-x}N_{63}P$ ($x=0$–16). Within the Broyden–Fletcher–Goldfarb–Shanno (BFGS) scheme [22], geometry optimization was performed under preselected space group allowing both cell parameter and internal coordinates relaxation.

3. Results and discussions

In our calculations, the band gap (E_g) of c-Si_3N_4 is 3.2 eV, close to the theoretical prediction of 3.45 eV [8] and the experimental result of 3.3 eV [23], but lower than the value of ~4.3 eV determined by a recent experiment [24]. In order to further demonstrate the applicability of our theoretical model in studying ternary nitride system, we performed calculations to test the site preference of C, Si and Ge in ternary nitride system. The spinel structure has two cation sites, which have tetrahedral (tet) and octahedral (oct) symmetry, respectively [9]. We calculated the enthalpy (H) of c-AB_5N_8 formula unit (f.u.) (A, $B=$ C, Si and Ge), using a 56-atom supercell with the formula $A_4B_{20}N_{32}$. Table 1 shows the difference of enthalpy ($H_d=H(\text{tet})-H(\text{oct})$) between the two structures in which A assumes two different cation sites. It can be found that Si favors oct sites and C favors tet sites in Si_3N_4–C_3N_4 because of the value of H_d for SiC_5N_8 (4.1 eV/f.u.) and for CSi_5N_8 (−1.9 eV/f.u.). This is in agreement with the theoretical prediction by Ching et al. [10]. It also can be found that Ge much prefers tet sites over oct sites, while Si prefers oct sites in Si_3N_4–Ge_3N_4 due to the value of H_d for $GeSi_5N_8$ (−0.6 eV/f.u.) and for $SiGe_5N_8$ (0.5 eV/f.u.). This is again well in agreement with the results of experiments [6] and the theoretical study [9]. All this consistency can demonstrate the accuracy of our method, which can be used to study the electronic properties of P-doped spinel systems.

Fig. 1 shows the calculated density of states (DOS) of the spinel system $C_xSi_{48-x}N_{63}P$ with C at tet sites and the P concentration of 1.56 percent, for a series of x-values. The 1.56% of P concentration results from substituting one P atom with N in a 112-atom supercell. There is only one anion site in spinel structure, so substitution of one P atom with N need not consider the site preference. As x increases, a large band-gap (E_g) reduction is observed. The x-dependence of E_g (Fig. 2) is not linear. At $x=13$, the gap disappears and an insulator-to-metal transition is realized. Beyond $x=13$, this solid solution is a metal all the way up to $x=16$. A similar insulator-to-metal transition by replacing Si by Ti of the spinel structure has been predicted by Ching et al. due to the "impurity bands" (introduced by Ti atom) growing and merging with the conduction bands [11]. It is well known that both GGA and LDA band gaps are not accurate enough to be able to explain experimental data well, but the predicted pressure dependence of band gap is in good agreement with experiment [25]. In order to find the origin of the large band-gap reduction in c-$(Si,C)_3N_4$:P, we calculated pressure dependence of GGA band-gap variations of a few

Table 1
Calculated difference of enthalpy H_d (eV/f.u.) $=H(\text{tet})-H(\text{oct})$ of c-AB_5N_8 between the two structures in which A assumes two different cation sites

	SiC_5N_8	CSi_5N_8	$GeSi_5N_8$	$SiGe_5N_8$
H_d	4.1	−1.9	−0.6	0.5

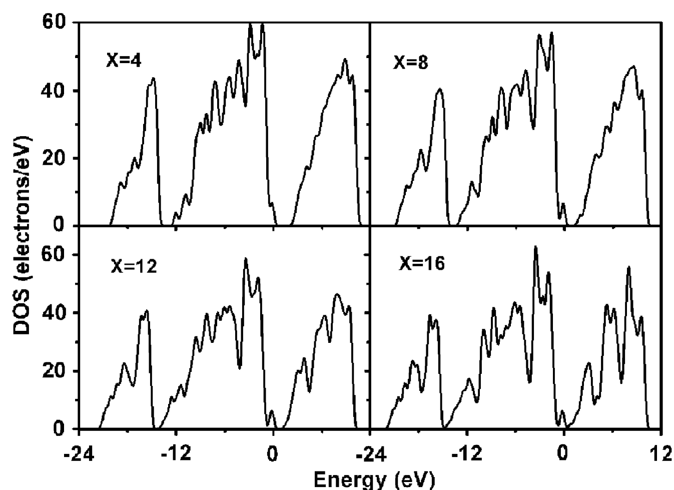

Fig. 1. Density of states (DOS) spectra of $C_xSi_{48-x}N_{63}P$ for a series of x-values.

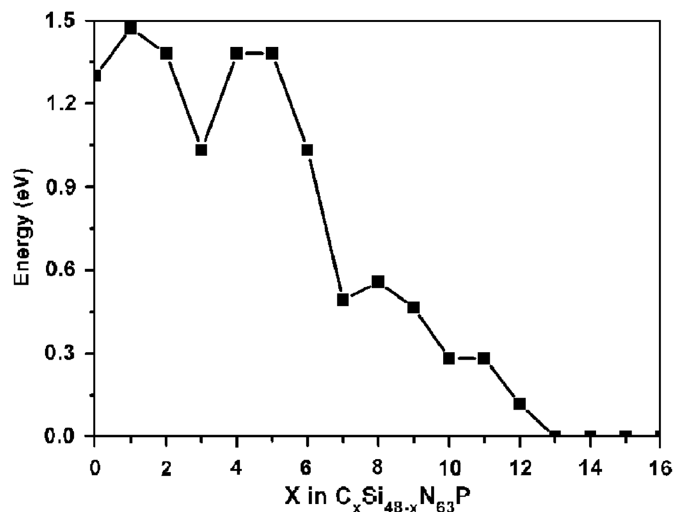

Fig. 2. Band-gap energy of $C_xSi_{48-x}N_{63}P$ as a function of x. The solid line is a guide to the eye.

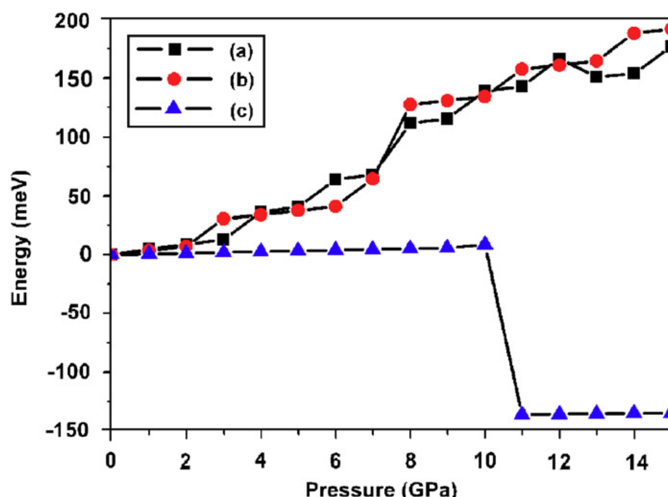

Fig. 3. Change of the band-gap variations of (a) $Si_{24}N_{32}$, (b) $CSi_{23}N_{32}$, and (c) $Si_{24}N_{31}P$ as a function of pressure. The solid line is a guide to the eye.

samples shown in Fig. 3. In the case of c-Si_3N_4, E_g increases nonlinearly with increasing pressure. A similar behavior is observed for the system of $CSi_{23}N_{32}$, which indicates that substitution Si with C in c-Si_3N_4 will not change the nature of band structure greatly. Adding P, however, greatly changes the pressure dependence. The system of $Si_{24}N_{31}P$ shows pressure independence of E_g between 0 and 10 GPa, and a sharp decrease of ~145 meV at 11 GPa. Beyond 11 GPa, there is also pressure independence of E_g. The pronounced change in the pressure dependence of E_g by substitutional P can be understood in terms of a pressure-induced transformation of the nature of the valence band maximum, namely, from more extended states to more localized states.

To examine the degree of localization of these valence band maximum states, in Fig. 4, we plot the total DOS (TDOS) and partial DOS (PDOS) spectra of the structure $C_8Si_{40}N_{63}P$. In Fig. 4, at the valence band maximum (energy = ~0 eV), the *p*-component of TDOS increases clearly. Meanwhile, it is interesting to find that the PDOS of P is the only state that mainly locates at the valence band maximum. The conduction bands originate mainly from the contribution of 2*p* orbitals of C atoms (donated 2*p*(C)) and 3*s*3*p* orbitals of Si (donated 3*s*3*p*(Si)). The valence band between −20.5 and −14.5 eV is mainly composed of 2*s* orbitals of N (donated 2*s*(N)). The major contribution to valence band between −13.0 and 0 eV comes from 2*p*(N), 2*p*(C), 3*p*(Si) and 3*p* orbitals of P (donated 3*p*(P)). The electronic density near the valence band maximum mainly consists of the contribution of 3*p*(P). So, it is clear that the increase of TDOS at the valence band maximum is introduced by the P impurity.

Here, we provide some possible explanations for the E_g reduction and its potential applications. First, 2*p*(C) and 2*p*(N) are likely to make stronger hybridization than 3*p*(Si) and 2*p*(N) because of the smaller energy difference between 2*p* orbital of C and N. Likely, 3*p*(Si) and 3*p*(P) form

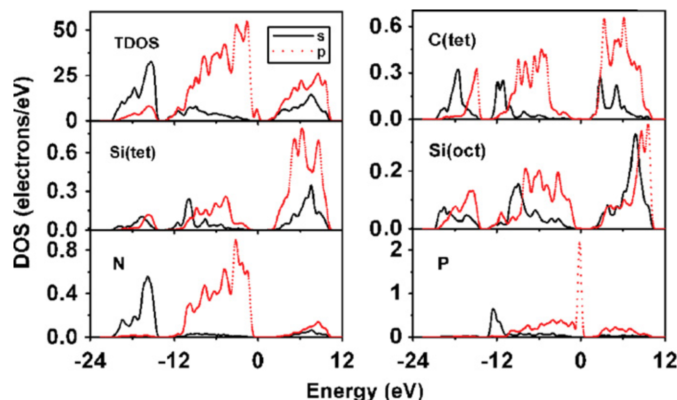

Fig. 4. Density of states (DOS) spectra of the structure with the formula $C_8Si_{40}N_{63}P$.

stronger hybridization than 3*p*(Si) and 2*p*(N) because of the same reason, together with the more extended 3*p*(P) orbital compared with 2*p*(N). Thus, when substituting Si by C in c-Si_3N_4, the stronger 2*p*(C)–2*p*(N) hybridization will reduce the 3*p*(Si)–2*p*(N) hybridization. This will enhance the 3*p*(Si)–3*p*(P) hybridization. This stronger 3*p*(Si)–3*p*(P) hybridization pushes the 3*p*(Si) level upward and the valence band top as well to a higher energy. Second, electronegativity may play an important role in the E_g reduction. The electronegativities of N, C, P, and Si are 3.04, 2.55, 2.19, and 1.90, respectively [26]. Since the electronegativity describes the ability of an atom to attract electrons to itself, it is expected that the valence electrons in Si–N or C–N bonds will be attracted strongly by the N atoms which was confirmed by first-principles calculations [8,10]. P has a smaller electronegativity and therefore is more willing to donate electrons to C in c-$(Si,C)_3N_4$:P. This may be the reason for the E_g reduction with increasing C. With the desirable E_g and an insulator-to-metal transition at a suitable C-to-Si ratio, the c-$(Si,C)_3N_4$:P has potential applications in certain semiconductor technology where the size of the gap plays a crucial role. And with the proper ratio of C to P, this spinel phase can be lattice matched to c-Si_3N_4, which allows the design of multi-junction devices.

In summary, by first-principles pseudopotential calculations, it is predicted that when Si is substituted with C at tet sites in c-Si_3N_4:P, the band gap can be adjusted, and an insulator-to-metal transition will occur at the C-to-Si ratio of 0.27. The pronounced change of the pressure dependence of band-gap variation in c-Si_3N_4:P indicates that adding of P can greatly change the nature of band structure. From the DOS spectra, it is observed that the TDOS increases at the valence band maximum, which originates from the contribution of 3*p* orbitals of P. Finally, some potential applications are discussed.

Acknowledgments

This work was supported by the National Natural Science Foundation of China (NSFC, no. 20473046) and

Research Program of Ministry of Science and Technology (2005CCA00900).

References

[1] A. Zerr, G. Miehe, G. Serghiou, M. Schwarz, E. Kroke, R. Riedel, H. Fueß, P. Kroll, R. Boehler, Nature (London) 400 (1999) 340.
[2] T. Sekine, J. Am. Ceram. Soc. 85 (2002) 113.
[3] G. Serghiou, G. Miehe, O. Tschauner, A. Zerr, R. Boehler, J. Chem. Phys. 111 (1999) 4659.
[4] K. Leinenweber, M. O'Keeffe, M.S. Somayazulu, H. Hubert, P.F. McMillan, G.H. Wolf, Chem. Eur. J. 5 (1999) 3076.
[5] N. Scotti, W. Kockelmann, J. Senker, S. Traßel, H. Jacobs, Z. Anorg. Allg. Chem. 625 (1999) 1435.
[6] E. Soignard, P.F. McMillan, K. Leinenweber, Chem. Mater. 16 (2004) 5344–5349.
[7] T. Sekine, T. Mitsuhashi, Appl. Phys. Lett. 79 (2001) 2719.
[8] S.-D. Mo, L. Ouyang, W.Y. Ching, I. Tanaka, Y. Komyama, R. Riedel, Phys. Rev. Lett. 83 (1999) 5046.
[9] J. Dong, J. Deslippe, O.F. Sankey, E. Soignard, P.F. McMillan, Phys. Rev. B 67 (2003) 094104.
[10] W.Y. Ching, S.-D. Mo, I. Tanaka, M. Yoshiya, Phys. Rev. B 63 (2001) 064102.
[11] W.Y. Ching, S.-D. Mo, L. Ouyang, I. Tanaka, M. Yoshiya, Phys. Rev. B 61 (2000) 10609.
[12] P. Kroll, J. Solid State Chem. 176 (2003) 530.
[13] A. Zerr, R. Riedel, T. Sekine, J.E. Lowther, W.Y. Ching, I. Tanaka, Adv. Mater. 18 (2006) 2933.
[14] J.I. Pankove, J.A. Hutchby, J. Appl. Phys. 47 (1976) 5387.
[15] L. Bellaiche, S.-H. Wei, A. Zunger, Appl. Phys. Lett. 70 (1997) 3558.
[16] J.B. Li, L.W. Wang, Phys. Rev. B 67 (2003) 033102.
[17] W. Kohn, L.J. Sham, Phys. Rev. 140 (1965) A1133.
[18] M.C. Payne, M.P. Teter, D.C. Allan, T.A. Arias, J.D. Joannopoulos, Rev. Mod. Phys. 64 (1992) 1045.
[19] D. Vanderbilt, Phys. Rev. B 41 (1990) 7892.
[20] J.P. Perdew, K. Burke, M. Ernzerhof, Phys. Rev. Lett. 77 (1996) 3865–3868.
[21] H.J. Monkhorst, J.D. Pack, Phys. Rev. B 13 (1976) 5188.
[22] E. Polak, Computational Methods in Optimization, Academic Press, New York, 1971, p. 56.
[23] A. Zerr, et al., Acta Crystallogr. A 58 (2002) C47.
[24] S. Leitch, A. Moewes, L. Ouyang, W.Y. Ching, T. Sekine, J. Phys.: Condens. Matter 16 (2004) 6469.
[25] E.D. Jones, N.A. Modine, A.A. Allerman, S.R. Kurtz, A.F. Wright, S.T. Tozer, X. Wei, Phys. Rev. B 60 (1999) 4430.
[26] J.J. Lagowski, Modern Inorganic Chemistry, Marcel Dekker, New York, 1973.